

# Life tables shape genetic diversity in marine fishes

Pierre Barry<sup>1</sup>, Thomas Broquet<sup>2</sup>, Pierre-Alexandre Gagnaire<sup>1</sup>

<sup>1</sup>ISEM, Univ Montpellier, CNRS, EPHE, IRD, Montpellier, France.

<sup>2</sup>CNRS & Sorbonne Université, UMR 7144, Station Biologique de Roscoff, 29680 Roscoff, France.

## Abstract

1

2 Genetic diversity varies among species due to a range of eco-evolutionary processes that  
3 are not fully understood. The neutral theory predicts that the amount of variation in the  
4 genome sequence between different individuals of the same species should increase with its  
5 effective population size ( $N_e$ ). In real populations, multiple factors that modulate the variance  
6 in reproductive success among individuals cause  $N_e$  to differ from the total number of individuals  
7 ( $N$ ). Among these, age-specific mortality and fecundity rates are known to have a direct impact  
8 on the  $\frac{N_e}{N}$  ratio. However, the extent to which vital rates account for differences in genetic  
9 diversity among species remains unknown. Here, we addressed this question by comparing  
10 genome-wide genetic diversity across 16 marine fish species with similar geographic distributions  
11 but contrasted lifespan and age-specific survivorship and fecundity curves. We sequenced the  
12 whole genome of 300 individuals to high coverage and assessed their genome-wide heterozygosity  
13 with a reference-free approach. Individual genome-wide heterozygosity varied from 0.2 to 1.4%,  
14 and adult lifespan was by far the most significant predictor of genetic diversity, with a large  
15 negative effect ( $slope = -0.089$  per additional year of lifespan) that was further increased when  
16 brooding species providing intense parental care were removed from the dataset ( $slope = -0.129$   
17 per additional year of lifespan). Using published vital rates for each species, we showed that the  
18  $\frac{N_e}{N}$  ratio only generated by life tables predict the observed differences in genetic diversity among  
19 species. We further found that the extent of reduction in  $\frac{N_e}{N}$  with increasing adult lifespan is  
20 particularly strong under Type III survivorship curves (high juvenile and low adult mortality)  
21 and increasing fecundity with age, which is typical of marine fish. Our study highlights the  
22 importance of vital rates in the evolution of genetic diversity within species in nature.

23 **Key words:** genetic diversity, life tables, adult lifespan, variance in reproductive success, ma-  
24 rine fishes

25

## Author Summary

26 Understanding how and why genetic diversity varies across species has important implica-  
27 tions for evolutionary and conservation biology. Although genomics has vastly improved our  
28 ability to document intraspecific DNA sequence variation at the genome level, the range and  
29 determinants of genetic diversity remain partially understood. At a broad taxonomic scale in  
30 eukaryotes, the main determinants of diversity are reproductive strategies distributed along a  
31 trade-off between the quantity and the size of offspring, which likely affect the long-term effec-  
32 tive population size. Long-lived species also tend to show lower genetic diversity, a result which  
33 has however not been reported by comparative studies of genetic diversity at lower taxonomic  
34 scales. Here, we compared genetic diversity across 16 European marine fish species showing  
35 marked differences in longevity. Adult lifespan was the best predictor of genetic diversity, with  
36 genome-wide average heterozygosity ranging from 0.2% in the black anglerfish to 1.4% in the  
37 European pilchard. Using life tables summarizing age-specific mortality and fecundity rates for  
38 each species, we showed that the variance in lifetime reproductive success resulting from age  
39 structure, iteroparity and overlapping generations can predict the range of observed differences  
40 in genetic diversity among marine fish species. We then used computer simulations to explore  
41 how combinations of vital rates characterizing different life histories affect the relationship bet-  
42 ween adult lifespan and genetic diversity. We found that marine fishes that display high juvenile  
43 but low adult mortality, and increasing fecundity with age, are typically expected to show re-  
44 duced genetic diversity with increased adult lifespan. However, the impact of adult lifespan  
45 vanished using bird and mammal-like vital rates. Our study shows that variance in lifetime  
46 reproductive success can have a major impact on a species' genetic diversity and explains why  
47 this effect varies widely across taxonomic groups.

## 48 Introduction

49 Genetic diversity, the substrate for evolutionary change, is a key parameter for species'  
50 adaptability and vulnerability in conservation and management strategies (Frankham, 1995;  
51 Lande, 1995). Understanding the determinants of species' genetic diversity has been, however,  
52 a long standing puzzle in evolutionary biology (Lewontin, 1974). Advances in DNA sequencing  
53 technologies have allowed describing the range of genetic diversity levels across eukaryote species  
54 and identifying main evolutionary processes underlying that variation (Leffler et al., 2012;  
55 Romiguier et al., 2014). But the extent and reasons for which life-history traits, and in particular  
56 reproductive strategies, influence genetic diversity remain to be clarified (Ellegren and Galtier,  
57 2016).

58 The neutral theory provides a quantitative prediction for the amount of genetic variation at  
59 neutral sites (Kimura, 1983). Assuming equilibrium between the introduction of new variants  
60 by mutations occurring at rate  $\mu$ , and their removal by genetic drift at a rate inversely pro-  
61 portional to the effective population size  $N_e$ , the amount of genetic diversity ( $\theta$ ) of a stable  
62 randomly mating population is equal to  $4N_e\mu$  (Kimura and Crow, 1964). This quantity should  
63 basically determine the mean genome-wide heterozygosity expected at neutral sites for any  
64 given individual in that population. However, since the neutral mutation-drift balance can be  
65 slow to achieve, contemporary genetic diversity often keeps the signature of past demographic  
66 fluctuations rather than being entirely determined by current population size. Therefore, gene-  
67 tic diversity should be well predicted by estimates of  $N_e$  that integrate the long-term effect of  
68 drift over the coalescent time. Unfortunately, such estimates are very difficult to produce using  
69 demographic data only.

70 Demographic variations set aside, the most proximate determinant of  $N_e$  is the actual num-  
71 ber of individuals ( $N$ ), also called the census population size. Comparative genomic studies in  
72 mammals and birds have showed that current species abundance correlates with the long-term  
73 coalescent  $N_e$ , despite potential deviation from long-term population stability in several of the  
74 species studied (Díez-Del-Molino et al., 2018; Leroy et al., 2020; Peart et al., 2020). General  
75 laws in ecology, such as the negative relationship between species abundance and body size  
76 (White et al., 2007) have also been used to predict the long-term  $N_e$ . Higher genetic diversity  
77 in small body size species was found in butterflies and Darwin's finches (Mackintosh et al.,  
78 2019; Brüniche-Olsen et al., 2019), while in the latter genetic diversity also positively correla-  
79 ted with island size, another potential proxy for the long-term  $N_e$  (Brüniche-Olsen et al., 2019).  
80 Surprisingly, however, genetic diversity variation across Metazoans is much better explained by  
81 fecundity and propagule size than classical predictors of species abundance such as body size  
82 and geographic range (Romiguier et al., 2014). This result has been attributed to differences  
83 among species with contrasted reproductive strategies in their long term probability of extinc-  
84 tion. Under this hypothesis, species with low fecundity and large propagule size ( $K$ -strategists)  
85 would be more resilient to low population size episodes compared to species with high fecundity  
86 and small propagule size ( $r$ -strategists) that would go extinct if they reach such population sizes  
87 (Romiguier et al., 2014). By contrast, Mackintosh et al. (2019) found no effect of propagule  
88 size on genetic diversity within Papilionidae, a family showing little variation in reproductive  
89 strategy. Therefore, the major effect of the  $r/K$  gradient on genetic diversity variation across  
90 Metazoa probably hides other determinants that act within smaller branches of the tree of life.  
91 In particular, the extent and mechanisms by which the complex interplay between demographic  
92 and evolutionary processes influence genetic variation remains unclear.

93 Other factors than fluctuations in population size are known to reduce the value of  $N_e$   
94 relative to the census population size, impacting the  $\frac{N_e}{N}$  ratio to different extent from one  
95 species to another. These factors include unbalanced sex-ratios, variance in lifetime reproductive  
96 success among individuals, age structure, kinship-correlated survival and some metapopulation



97 configuration (Wright, 1969; Falconer, 1989; Lande and Barrowclough, 1987). A potentially  
98 strong effect comes from variance in the number of offspring per parent ( $V_k$ ), which reduces  $N$   
99 following  $N_e = \frac{4N-4}{V_k+2}$  (Crow and Kimura, 1970). Variance in reproductive success can naturally  
100 emerge from particular age-specific demographic characteristics summarized in life tables that  
101 contain age- (or stage-) specific survival and fecundity rates (Ricklefs and Miller, 1999). The  
102 impact of life tables characteristics on expected  $\frac{N_e}{N}$  ratio has been the focus of a large body  
103 of theoretical and empirical works (Nunney, 1991, 1996; Waples, 2002, 2016b,a; Waples et al.,  
104 2018). Accounting for iteroparity and overlapping generations, a meta-analysis of vital rates  
105 in 63 species of plants and animals revealed that half of the variance in  $\frac{N_e}{N}$  among species can  
106 be explained by just two life-history traits, adult lifespan and age at maturity (Waples et al.,  
107 2013). Despite this high predictive power of life tables, there is still no attempt to evaluate the  
108 extent to which lifetime variance in reproductive success explains differences in genetic diversity  
109 between species with different life table components.

110 Marine fishes are good candidate to address this question. They are expected to display  
111 particularly high variance in reproductive success as a result of high abundance, type III sur-  
112 vivorship curves (i.e. high juvenile mortality and low adult mortality) and increasing fecundity  
113 with age. Consequently, it has been suggested that marine fish species show a marked discre-  
114 pancy between adult census size and effective population size, resulting in  $\frac{N_e}{N}$  ratios potentially  
115 smaller than  $10^{-3}$ . The disproportionate contribution of a few lucky winners to the offspring  
116 of the next generation is sometimes referred as the "big old fat fecund female fish" (BOFFFF)  
117 effect, a variant of the "sweepstakes reproductive success" hypothesis (Hedgecock, 1994; He-  
118 drick, 2005; Hedgecock and Pudovkin, 2011) that is often put forward to explain low empirical  
119 estimates of effective population sizes from genetic data Hauser and Carvalho (2008). However,  
120 subsequent theoretical work showed that low values of  $\frac{N_e}{N}$  below 0.01 can only be generated with  
121 extreme age-structure characteristics (Waples, 2016b). The real impact of lifetime variance in  
122 reproductive success on genetic diversity thus remains unclear, even in species like fish in which  
123 its impact is supposed to be strong. Contrasting results have been obtained by comparative  
124 studies in marine fishes, including negative relationship with body size (Pinsky and Palumbi,  
125 2014; Waples, 1991), fecundity (Martinez et al., 2018) and overfishing (Pinsky and Palumbi,  
126 2014). However, these studies relied on few nuclear markers, known to provide inaccurate or  
127 biased estimates of genetic diversity (Väli et al., 2008), and compared species sampled from  
128 different locations, thus, likely having different demographic histories, which could blur the  
129 relationship between species characteristics and genetic diversity (Ellegren and Galtier, 2016).

130 Here, we compared the genome-average heterozygosity to the life history traits and life  
131 table characteristics of 16 marine teleostean species sharing a similar Atlantic and Mediterra-  
132 nean distributions. We estimated genetic diversity from unassembled whole-genome reads using  
133 **GenomeScope** (Vurtture et al., 2017) and checked the validity of these estimates with those obtai-  
134 ned using a high-standard reference-based variant calling approach. Using this data, we related  
135 species genetic diversity to eight simple quantitative and qualitative life history traits. Then,  
136 we built estimates of species life tables and determined if the lifetime variance in reproductive  
137 success induced by these tables could explain observed differences in genetic diversity using an  
138 analytical and a forward-in-time simulation approach. Finally, we generalized our findings by  
139 exploring the influence of age-specific survival and fecundity rates on variance in reproductive  
140 success and ultimately genetic diversity via simulated lifetimes tables.

## 141 **Material and Methods**

### 142 **Sampling and DNA extraction**

143 We sampled 16 marine teleostean fish species presenting a wide diversity of life-history  
144 strategies expected to affect genetic diversity (Table S2). All these species share broadly over-  
145 lapping distributions across the northeastern Atlantic and Mediterranean regions. Sampling  
146 was performed at the same four locations for all species: two in the Atlantic (the Bay of Biscay  
147 in southwestern France or northwestern Spain and the Algarve in Portugal), and two in the  
148 western Mediterranean Sea (the Costa Calida region around Mar Menor in Spain and the Gulf  
149 of Lion in France see Fig 1A). For 12 of these species, 20 individuals were sampled (5 per  
150 location). For the 4 other species the total number of samples ranged from 10 to 19 (Table  
151 S2). Individuals were either sampled from landings in local fish markets, captured in the field  
152 (using hand nets, lure fishing, spearfishing or beach seines) or provided by collaborators. The  
153 majority of the sampling was done in 2018 and 2019. Whole-genomic DNA was extracted from  
154 fin or tissue clips stored in 95% ethanol using the NucleoSpin Tissue Kit (Macherey-Nagel), and  
155 treated with RNase A to remove residual RNA. Double-stranded nucleic acid concentration  
156 was quantified using Qubit2.0 and standardized to 20ng per  $\mu$ l.

### 157 **Whole-genome sequencing and reads quality control**

158 Individual whole-genome sequencing libraries were prepared following the Illumina TruSeq  
159 DNA PCR-Free Protocol and sequenced by Genewiz Inc (USA). Libraries were quantified and  
160 multiplexed by groups of 40 individuals and sequenced on two S4 flow cells on a NovaSeq6000  
161 instrument (Illumina) to generate 150 pb paired-end reads, targetting an average read depth  
162 of 20X per individual. Raw reads were preprocessed with `fastp` v.0.20.0 (Chen et al., 2018)  
163 using default parameters, allowing quality control, filtering by quality, length and complexity,  
164 and adapter trimming to be performed in a single step. Base correction was performed using  
165 quality comparison between overlapping bases of paired-end reads, and polyG tail trimming  
166 was enabled to correct for artefactual G repetitions occurring in Novaseq read tails.

### 167 **Estimation of genetic diversity**

168 We used `GenomeScope` v.1.0 to estimate individual genome-wide heterozygosity (Vurture  
169 et al., 2017). Briefly, this method uses a  $k$ -mers based statistical approach to infer overall  
170 genome characteristics, including total haploid genome size, percentage of repeat content and  
171 genetic diversity from unassembled short read sequencing data. Provided a sufficient average  
172 coverage depth (e.g. 20X), `GenomeScope` evaluates the fraction of heterozygous sites from the  
173 ratio of the height of the heterozygous to the homozygous  $k$ -mer peak, occurring at 50% (i.e.  
174 10X) and 100% (i.e. 20X) of the average coverage depth, respectively. We used `jellyfish`  
175 v.2.2.10 to compute the  $k$ -mer profile of each individual (Marçais and Kingsford, 2011). The  
176 number of different possible  $k$ -mers (and thus the precision of the method) increases with  $k$ ,  
177 but so does the runtime and the probability of "wrong"  $k$ -mers due to sequencing errors. We  
178 set  $k = 21$  as recommended by `GenomeScope` and performed a sensitivity analysis by estimating  
179 genetic diversity and genome size for one individual of *D. labrax* using  $k$  from 17 to 25 (Fig S3).  
180 The genetic diversity of each species was determined as the median of the individual genome-  
181 wide heterozygosity values. We chose the median instead of the mean diversity since it is less  
182 sensitive to the possible presence of individuals with abnormal genetic diversity values (e.g.  
183 inbred or hybrid individuals) in our samples.

184 In order to assess the reliability of `GenomeScope` and detect potential systematic bias, we  
185 compared our results with high-standard estimates of genetic diversity obtained after read ali-

186 gnement against available reference genomes. To perform this test, we used the sea bass (*D.*  
187 *labrax*) and the European pilchard (*S. pilchardus*), two species that represent the lower and  
188 upper limits of the range of genetic diversity in our dataset (Table S2, Fig 1D). The 20 re-  
189 sequenced genomes for each of these two species were aligned with `bwa-mem` v.0.7.17 (Li and  
190 Durbin, 2009) to the reference genomes retrieved from Louro et al. (2019) and Tine et al.  
191 (2014) for *S. pilchardus* and *D. labrax*, respectively. We then removed PCR duplicates with the  
192 Picard tools `MarkDuplicates` v.2.23.2. We followed the best-practice pipeline in `GATK` v.4.1.6.0  
193 for variant calling (Poplin et al., 2018): we ran `HaplotypeCaller` with default options to ge-  
194 nerate individual GVCFs files, stored them in a database with `GenomicsDBImport` and finally  
195 computed VCF files with `GenotypeGVCFs`. We didn't apply post variant calling filtering steps,  
196 such as hard filters on genotype quality scores or Hardy-Weinberg Equilibrium criterion, in  
197 order to avoid potential bias in the comparison of genetic diversity between species with very  
198 different rates of heterozygosity. However, we assume that possible bias due to the absence of  
199 variant filtering should not impact differences among individuals within each species. Finally,  
200 the VCF files generated with `GATK` were analyzed with `vcftools` v.0.1.17 (Danecek et al., 2011)  
201 to compute individual genome-wide heterozygosity.

## 202 Life history traits database

203 We collected seven simple quantitative variables describing various aspects of the biology and  
204 ecology of the 16 species: body size, trophic level, fecundity, propagule size, age at maturity,  
205 lifespan and adult lifespan (Table S2 for detailed informations on bibliographic references).  
206 There was substantial variability in the values that we found for some of these traits. This  
207 variation could have different causes including plasticity, selective pressures or different metho-  
208 dologies. Although we did not take into account this variability, we aimed to take the most  
209 representative values reported for each species and each trait, as described below. In addition,  
210 we collected two qualitative variables describing the presence/absence of hermaphroditism and  
211 brooding behaviour, as revealed by male-pouching of eggs (*H. guttulatus* and *S. typhle*) or nest-  
212 guarding (*C. galerita*, *S. cinereus* and *S. cantharus*). As growth is indeterminate in fish, we  
213 defined adult body size as the infinite length,  $L_{inf}$  determined by the Von Bertalanffy equation  
214 ( $L_t = L_{inf}[1 - \exp^{-K(t-t_0)}]$ ), that links individual body size  $L_t$  to age  $t$ , with  $K$  a parameter  
215 defining the shape of this relationship (Pauly et al., 1987). We estimated adult body size as the  
216 median of all  $L_{inf}$  values reported for each species in the online database Fishbase (Froese et al.,  
217 2000). As  $L_{inf}$  was not documented in Fishbase for *D. puntazzo* and *C. galerita*, we took the  
218 median of the values reported in (Kraljević et al., 2007) and (Domínguez-Seoane et al., 2006)  
219 for *D. puntazzo*, and the maximum length observed in (Milton, 1983) for *C. galerita*. Trophic  
220 level was retrieved from Fishbase. Fecundity was defined as the absolute fecundity, i.e. the mean  
221 number of eggs in an ovary of a female in a single spawning event. Females may spawn several  
222 times during one reproductive season (Ganias et al., 2003; Murua and Motos, 2006), so absolute  
223 fecundity is not the value most directly relevant to global genetic diversity. However, it is the  
224 most commonly reported in the literature as the number of spawnings events per reproductive  
225 season is difficult to measure. Because fecundity is proportional to individual body size, we  
226 computed fecundity at infinite length,  $L_{inf}$ . Propagule size was determined following Romi-  
227 guier et al. (2014), as the size of the dispersal stage that becomes independent of the parents.  
228 For all species of this study, this corresponded to egg diameter, except for brooders, for which  
229 we used hatching size. All propagule size data were retrieved from species-specific references.  
230 Age at maturity was defined as the age at which 50% of the population is mature. Values for  
231 age at maturity were taken from Tsikliras and Stergiou (2015) for seven species while other  
232 values were retrieved from species-specific references. Likewise, lifespan values were taken from  
233 (Tsikliras and Stergiou, 2015) for six species and completed with specific references. Finally,

234 adult lifespan was defined as *Lifespan* – *Age at Maturity* (Waples et al., 2013).

## 235 Construction of life tables

236 Life tables summarize survival rates and fecundities at each age during the life of an in-  
237 dividual (Ricklefs and Miller, 1999). Thus, they provide detailed information on vital rates  
238 that influence the variance in lifetime reproductive success among individuals. This tool is well  
239 designed to describe population structure from the probability of survival to a specific age at  
240 which a specific number of offspring are produced. Ideally, age-specific survival is estimated  
241 by direct demographic measures, such as mark-recapture. Unfortunately, direct estimates of  
242 survival were not available for the 16 studied species. We thus followed Benvenuto et al. (2017)  
243 to construct species life tables. Age-specific mortality of species *sp*,  $m_{sp,a}$ , is a function of body  
244 length at age *a*,  $L_{sp,a}$ , asymptotic Von Bertalanffy length  $L_{inf}$ , and species Von Bertalanffy  
245 growth coefficient,  $K_{sp}$  :

$$m_{sp,a} = \left[ \left( \frac{L_{sp,a}}{L_{inf,sp}} \right) \right]^{-\frac{1}{5}} \times K_{sp} \quad (1)$$

246 Age-specific survival rates,  $s_{sp,a}$  were then estimated as :

$$s_{sp,a} = e^{-m_{sp,a}} \quad (2)$$

247 We collected age-specific length from empirical data and estimated  $L_{inf}$  and  $K$  values from  
248 age-length data as explained above, setting survival probability to zero at the maximum age  
249 (Appendix 1). When differences in age-specific lengths between sexes were suggested in the  
250 literature, we estimated a different age-specific survival curve for each sex. The relationship  
251 between absolute fecundity and individual length is usually well fitted with the power-law  
252 function ( $F = \alpha L^\beta$ ), although some studies also used an exponential function ( $F = \alpha e^{\beta L}$ ) or  
253 a linear function ( $F = \alpha + L\beta$ ). We collected empirical estimates of  $\alpha$  and  $\beta$  and determined  
254 age-specific fecundity from age-specific length and the fecundity-length function reported in the  
255 literature for each species. Fecundity was set to zero before the age at first maturity.

## 256 Variance in reproductive success and the $N_e/N$ ratio

257 To understand how differences in life tables drive differences in genetic diversity between  
258 species, we estimated the variance in lifetime reproductive success,  $V_k$  and the ensuing ratio  $\frac{N_e}{N}$   
259 using the analytic framework developed in **AgeNe** (Waples et al., 2011). **AgeNe** infers  $V_k$  using  
260 informations from life tables only. Hence, the variance in fecundity estimated is only generated  
261 by inter-individual differences in reproductive success and survival. **AgeNe** assumes constant  
262 population size, stable age structure, and no heritability of survival and fecundity. We used the  
263 life tables constructed as described above and set the number of new offsprings to 1000 per year.  
264 This setting is an arbitrary value which has no influence on the estimation of either  $V_k$  nor  $\frac{N_e}{N}$  by  
265 **AgeNe**. For all species, we set the initial sex-ratio at 0.5 and equal contribution of individuals  
266 of the same age (i.e. no sweepstake reproductive success among same-age individuals). We  
267 ran **AgeNe** and estimated  $\frac{N_e}{N}$  for each species. If genetic diversity differences among species  
268 are largely determined by differences in variance in reproductive success, we expect that the  
269 correlation between ratios of observed genetic diversity and ratios of  $\frac{N_e}{N}$  is well fitted by the  
270 line of equation  $y = x$ . To test this prediction, we fitted a linear model between the two ratios  
271 and tested if the estimated slope and intercept are different from 1 and 0, respectively, with a  
272 *t*-test.

273 Four life-history traits can generate differences in  $\frac{N_e}{N}$  between species: age at maturity, age-  
274 specific survival rates, age-fecundity relationships and sex-differences in these components. To



275 determine the role that each parameter plays in the differences in genetic diversity observed  
276 between species, we constructed alternative life tables where the effect of each parameter was  
277 removed one after the other. For example, to account for the effect of varying age at maturity  
278 on  $\frac{N_e}{N}$ , we constructed similar life tables as previously but with all species being mature at age  
279 1. To test the effect of varying survival rates between ages, we followed Waples (2016b) and  
280 calculated constant survival rates in order to have 0.01 percent of individuals remaining at the  
281 maximum age. To test the effect of increasing fecundity with age, we set constant fecundity for  
282 all ages. Finally, to test the effect of sex-differences in life tables, we constructed identical life  
283 tables for both males and females. For each of the 16 alternative life tables, we then tested if  
284 the linear relationship between pairwise-ratios of observed genetic diversity and  $\frac{N_e}{N}$  values are  
285 well-fitted by a model with slope equals to 1 and intercept 0, as previously.

## 286 Forward simulations

287 A complementary analysis of the contribution of life table properties on genetic diversity  
288 was performed using forward simulations in SLiM v.3.3.1 (Haller and Messer, 2017). Stochastic  
289 forward simulations allow a different formalisation compared to the deterministic model  
290 implemented in AgeNe. Thus, they provide another approach to the problem, which can be  
291 more intuitive to understand why vital rates affect  $N_e$  over the long-term, and ultimately ge-  
292 netic diversity. We simulated populations with overlapping generations, sex-specific lifespan,  
293 and age- and sex-specific fecundity and survival. We used life tables estimated as previously,  
294 and sex-specific lifespan estimates were collected in the literature as described above. For each  
295 individual, the number of offspring produced per year was determined by a Poisson distribu-  
296 tion with mean  $\lambda_{S,a}$  specific to each species and each age. Age at first maturity was set to 1  
297 for all simulations. Age and species-specific fecundity was determined as previously and scaled  
298 between 0 (age 0) and 100 (maximum age) within each species. In the simulations, each indi-  
299 vidual first reproduce and then either survive to the next year or die following a probability  
300 determined by its age and the corresponding life table. To keep population size constant in  
301 these non Wright-Fisher forwards simulations, we introduced a carrying capacity parameter,  
302 allowing population size to fluctuate around this capacity (Fig S15 - S22). We arbitrarily set  
303 this parameter to  $N = 2000$ , and simulated non-recombining 1Mb loci with a mutation rate of  
304  $\mu = 1e^{-7}$ . Each simulation was run for 25000 years, which was long enough for genetic diversity  
305 to reach mutation-drift equilibrium (Fig S23 - S30). For each simulation, we estimated the  
306 mean genetic diversity (i.e., the proportion of heterozygous sites along the 1Mb locus) over the  
307 last 10000 years after checking that an equilibrium has been reached. For each species, we ran  
308 50 replicates and defined the genetic diversity predicted by a given simulation scenario as the  
309 mean genetic diversity at equilibrium averaged over the 50 replicates.

310 As previously, we evaluated the contribution of each component among 8 alternative life  
311 tables by testing the linear relationship between observed and simulated ratios of genetic di-  
312 versity between pairs of species, and testing if the estimated slope and intercept differed from  
313 1 and 0, respectively.

## 314 Evaluating the impact of life tables beyond marine fish

315 To generalize our understanding of the influence of life tables on genetic diversity beyond  
316 the species used in this study, we simulated a wide range of age-specific survival and fecundity  
317 curves and explored their effect on the relationship between adult lifespan and variance in  
318 reproductive success. To this end, we defined 16 theoretical species with age at first maturity  
319 and lifespan equal to that of our real species and then we introduced variation in survival and  
320 fecundity curves to a set of 16 species. First, age-specific mortality was simulated following

321 Pinder et al. (1978) :

$$M(\text{Age}, \text{Age} + 1) = 1 - \exp\left(\frac{\text{Age}}{b}\right)^c - \left(\frac{\text{Age}+1}{b}\right)^c \quad (3)$$

322 where the value of  $c$  defines the form of the survivorship curve, with  $c > 1$ ,  $c = 1$  and  
323  $c < 1$  defining respectively a *Type I* (e.g. mammals), *Type II* (e.g. birds) and *Type III* (e.g.  
324 fish) survival curves. We took values of  $c$  from 0.01 to 30 (Fig 4A). Parameter  $b$  was equal to  
325  $-\frac{\text{Lifespan}}{\log(0.01)^{1/c}}$  to scale survivorship curves in such a way that 1% of the initial population remains  
326 at maximum age.

327 Second, age-specific fecundity was simulated with two models: constant and exponential. In  
328 the first model, fecundity is constant for all ages since maturity. In the second model, fecundity  
329 increases or decreases exponentially with age following  $F_{\text{Age}} = \exp^{f \times \text{Age}}$ , as it is often observed  
330 in marine fishes (Curtis and Vincent, 2006). For all simulations, we scaled maximum fecundity  
331 to 1 and took values of  $f$  ranging from  $-1$  to  $1$  (Fig 4A).

332 For each combination of  $c$  and  $f$ , and for each fecundity model, we simulated all species  
333 life tables given age at maturity and lifespan. Then, we ran `AgeNe` and estimated  $\frac{N_e}{N}$  for each  
334 simulated species and estimated the slope of the regression between adult lifespan and  $\frac{N_e}{N}$  across  
335 all 16 species.

336 We then explored the impact of alternative fecundity-age models on the relationship between  
337 adult lifespan and  $\frac{N_e}{N}$  using three additional biologically realistic models: linear ( $F_{\text{Age}} = a \times$   
338  $\text{Age} + b$ ), polynomial ( $F_{\text{Age}} = [\text{Age} - \text{AgeMat}][(\text{AgeMat} + \text{Lifespan} - \text{Age})^2]$ , common in  
339 mammal) (Gage, 2001) and power-law ( $F_{\text{Age}} = \text{Age}^f$ ). For the linear and the polynomial model,  
340  $f$  describes the maximum fecundity at lifespan and age with the highest fecundity, respectively  
341 (i.e. higher absolute values of  $f$  correspond to higher differences in fecundity between low and  
342 high fecund ages for both models).  $f$  lied from  $-1$  to  $1$  for the linear and the polynomial model.  
343 For the power-law model, we took values of  $f$  from  $-5$  to  $5$ .

## 344 Intraspecific variation in genetic diversity

345 We addressed the potential effects of population structure, demography and historical  
346 contingencies on genetic diversity by examining the extent of spatial variation in genetic diver-  
347 sity between the four populations within each species. First, we evaluated the relative amount  
348 of intraspecific compared to interspecific variation in genetic diversity. Then, we applied a  $z$ -  
349 transformation of individual genetic diversity within each species to put differences in species  
350 diversity on the same scale. We finally performed a hierarchical clustering analysis of the ma-  
351 trix of  $z$ -transformed genetic diversity values with `pheatmap` function available in `pheatmap`  
352 `v1.0.12` R package.

## 353 Statistical analyses

354 All statistical analyses were carried out using `R-3.6.1` (R Core Team, 2018). We fitted beta  
355 regression model between genetic diversity and any covariate with the R-package `betareg` v.3.1-  
356 3 (Cribari-Neto and Zeileis, 2010). We tested statistical interactions between any quantitative  
357 and qualitative covariates using likelihood tests with the `lmtest` v.0.9-37 package (Zeileis and  
358 Hothorn, 2002).

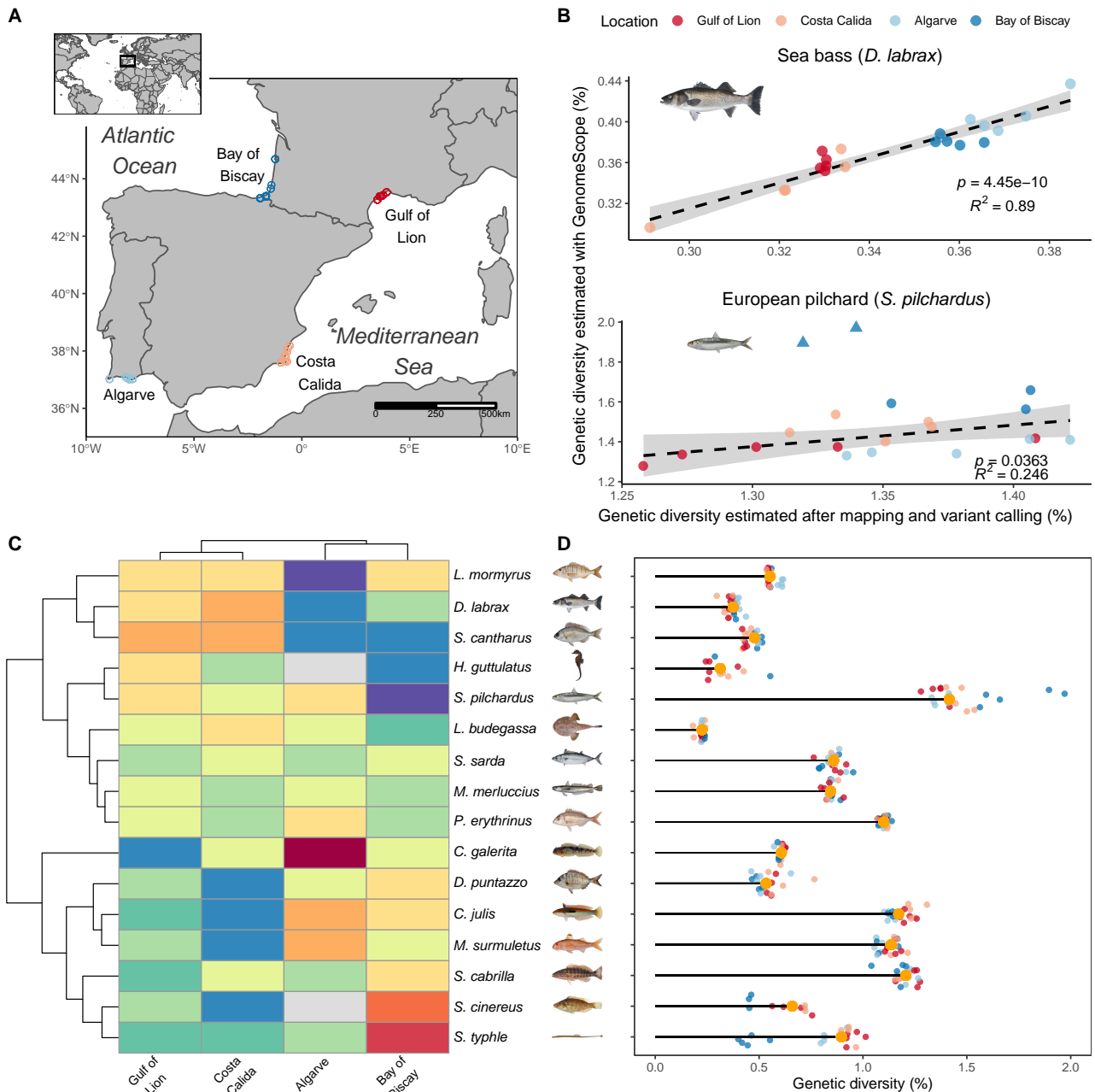


**FIGURE 1 – Sampling and estimation of genetic diversity in 16 marine fish species** - In panels A, B and D, the geographical origin of samples is represented by colors. Atlantic: Bay of Biscay (dark blue), Faro region in Algarve (light blue). Mediterranean: Murcia region in Costa Calida (pink), Gulf of Lion (red). **(A)** Sampling map of all individuals included in this study. Each point represents the coordinates of a sample taken from one of four locations: two in the Atlantic Ocean and two in the Mediterranean Sea. **(B)** Relationship between individual mean genome-wide heterozygosity estimated with the k-mer based reference-free approach in GenomeScope ( $y$ -axis), and the high standard reference-based approach in GATK ( $x$ -axis), for european sea bass (*D. labrax*, top) and european pilchard (*S. pilchardus*, bottom), regression made on circle points only, see text). **(C)** Heatmap clustering showing the variance in genetic diversity within species among locations. Each line represents one species, with the corresponding species name written on the right side; every column represents one location. Blue and red colors respectively indicate higher and lower genetic diversity within a location for a given species compared to the average species genetic diversity. **(D)** The range of individual genetic diversity within each species compared to the median genetic diversity represented with an orange dot. Species illustrations were retrieved from Iglésias (2013) with permissions.

## 359 Results

### 360 Whole-genome resequencing data set

361 We resequenced 300 individual genomes from 16 marine teleostean species, generating from  
362  $59.86 \times 10^6$  to  $200.92 \times 10^6$  reads per individual (mean =  $129 \times 10^6$ , sd =  $20 \times 10^6$ , Fig S1). The  
363 read quality score (Q30 rate) ranged between 88% and 94% (mean = 92.4%, sd = 1.1) and the  
364 duplication rate lied between 5 and 15% (mean = 10.8%, sd = 2.6) (Fig S1). GC content was  
365 moderately variable among species and highly consistent among individuals of the same species,  
366 except for one individual of *S. cabrilla*, *D. puntazzo* and *M. surmuletus* that showed a marked  
367 discrepancy with the overall GC content of their species (Fig S1). These three individuals were  
368 thus removed from downstream analyses to avoid potential issues due to contamination or poor  
369 sequencing quality (see discussion).

### 370 Estimation of genetic diversity with GenomeScope

371 The GenomeScope model successfully converged for all of the 297 individual genomes retained  
372 (Fig S4E). Estimated genome sizes were very consistent within species (Fig S4A-C). Estimated  
373 levels of genetic diversity were homogeneous within species with some few exceptions (e.g. *S.*  
374 *cinereus* and *S. typhle*) and most of the variability in genetic diversity was observed between  
375 species (Fig 1D). Two individuals (one *D. puntazzo* and one *P. erythrinus*) showed a surpris-  
376 ingly high genetic diversity (more than twice the average level of their species), indicating  
377 possible issues in the estimation of genome-wide heterozygosity. Therefore we removed these  
378 individuals from subsequent analysis, although their estimated genome size and GC content  
379 matched their average species values (therefore excluding contamination as a cause of genetic  
380 diversity estimation failures).

381 Observed values of genetic diversity ranged from 0.225% for *L. budegassa* to 1.415% for *S.*  
382 *pilchardus*. We found no correlation between species genetic diversity and genome size ( $p$ -  
383 *value* = 0.983). The estimation of genetic diversity was robust to the choice for  $k$ -mer lengths  
384 ranging from 21 to 25, suggesting a low sensibility of GenomeScope regarding this parameter (Fig  
385 S3). The fraction of reads mapped against reference genomes ranged between 96.72 and 98.50%  
386 for *D. labrax* and between 87.45 and 96.42 % for *S. pilchardus* (Table S1; Fig S2). Individual  
387 genetic diversity estimated with GenomeScope was significantly positively correlated to that  
388 estimated with the GATK reference-based variant calling approach for the two control species  
389 (Fig 1B). The geographic variance in genome-wide heterozygosity among individuals was very  
390 well captured for the sea bass (*D. labrax*,  $R^2 = 89\%$ ,  $p$ -*value* =  $4.45e^{-10}$ , Fig 1B) but less  
391 accurately for *S. pilchardus* ( $R^2 = 24.6\%$ ,  $p$ -*value* = 0.0363, Fig 1B), in which two individuals  
392 suffered from biased estimates. Although this comparison indicated a possibly lower accuracy  
393 of GenomeScope in the presence of very high heterozygosity values, the range of heterozygosities  
394 estimated by GenomeScope was highly similar to that estimated with GATK for the two control  
395 species. Thus, the detection of fine-scale variation among individuals within two species lying  
396 at opposite ends of a diversity gradient confirms that GenomeScope is well-suited to quantify  
397 genetic diversity differences among the 16 species in our dataset.

### 398 Adult lifespan is the best predictor of genetic diversity

399 We evaluated the effect of several key life history traits that potentially affect species genetic  
400 diversity (Table 1).

401 Two widely used predictors of population size, body size and trophic level, were not signi-  
402 ficantly correlated to genetic diversity ( $p$ -*value* = 0.119 and 0.676 respectively, Fig S6A-B).  
403 Although we detected a significant negative relationship between the logarithm of fecundity



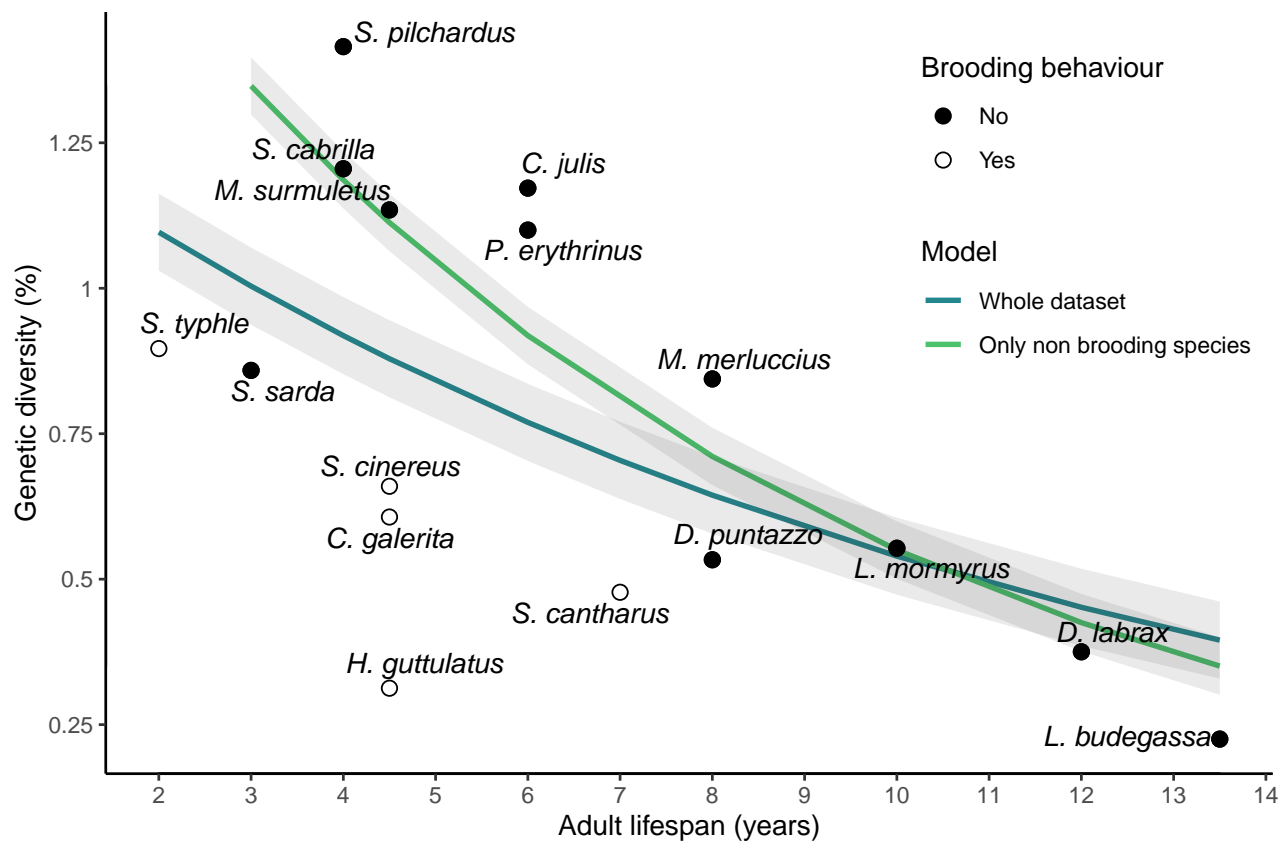


FIGURE 2 – **Relationship between species median genetic diversity (%) and adult lifespan** - Each point represents the median of observed genetic diversity among species' individuals samples. Adult lifespan is defined as the difference between lifespan and age at first maturity in years. Dot points represents non-brooding species, empty circles, brooding species. Dashed blue line and solid green line represent the beta regression between adult lifespan and genetic diversity considering either the whole dataset (16 species), or the 11 non-brooding species only, respectively.

404 and propagule size ( $p$ -value = 0.00131, slope =  $-0.4385 \pm 0.1076$ ) as in Romiguier et al. (2014),  
405 we found no significant correlation between either propagule size ( $p$ -value = 0.561), or the  
406 logarithm of fecundity ( $p$ -value = 0.785) and genetic diversity (Fig S6C-D).

407 By contrast, both lifespan ( $p$ -value = 0.011) and adult lifespan ( $p$ -value = 0.007) were signi-  
408 ficatively negatively correlated with genetic diversity (Table 1, Fig 2, Fig S6E). The percentage  
409 of variance explained by each variable reached 43.8 and 42.9 %, respectively.

410 We found no significant interaction between hermaphroditism and any of the previous va-  
411 riables on genetic diversity. By contrast, parental care showed a significant interaction with  
412 lifespan ( $p$ -value = 0.0011), adult lifespan ( $p$ -value = 0.0008) and body size ( $p$ -value = 0.0035)  
413 on genetic diversity. Brooding species (nest protection for *C. galerita*, *S. cinereus* and *S. cantha-*  
414 *rus* and male-pooch for *H. guttulatus* and *S. typhle*) had systematically lower genetic diversity  
415 than non-brooding species with similar lifespan.

416 When considering only non-brooding species, we found steeper negative correlations and hi-  
417 gher percentages of between-species variance in genetic diversity explained by lifespan ( $p$ -value =  
418  $1.017e^{-7}$ , pseudo- $R^2 = 0.851$ ) and adult lifespan ( $p$ -value =  $1.645e^{-7}$ , pseudo- $R^2 = 0.829$ , Fig  
419 1, Table 1). To test the relevance of considering this sub-dataset, we estimated the slope of the  
420 regression and the pseudo- $R^2$  for all combinations of 11 out of 16 species and compared the  
421 distribution of these values to the estimated slope and pseudo- $R^2$  obtained for the 11 non broo-  
422 ding species (Fig S11). The estimated slope for non brooders lied outside of the 95% confidence  
423 interval of the distribution of estimated slopes (slope =  $-0.129$ , 95% CI =  $[-0.122, -0.049]$ )  
424 and pseudo- $R^2$  (pseudo- $R^2 = 0.829$ , 95% CI =  $[0.073, 0.727]$ ). Furthermore, considering non-  
425 brooding species only, there was still no significant correlation between genetic diversity and tro-  
426 phic level ( $p$ -value = 0.259), propagule size ( $p$ -value = 0.170), and fecundity ( $p$ -value = 0.390),  
427 but genetic diversity appeared significantly correlated to body size ( $p$ -value =  $6.602e^{-5}$ , pseudo-  
428  $R^2 = 0.616$ ). We did not detect any significant correlation between any trait variable and genetic  
429 diversity within the sub-dataset of brooding species. However, this should be taken with caution  
430 given the very low number of brooding species ( $n = 5$ ) in our dataset.

431 Body size and lifespan were highly positively correlated traits in our dataset ( $p$ -value =  
432 0.00126,  $R^2 = 0.536$ , Fig S5). Thus, using empirical observations only, it was not possible to  
433 fully disentangle the impact of each of these traits among the possible determinants of genetic  
434 diversity in marine fishes. However, we found important differences in effect sizes for body size  
435 (slope =  $-0.014$ ), lifespan ( $-0.095$ ) and adult lifespan ( $-0.129$ ), which rule out body size as a  
436 major determinant of diversity in our dataset.

## 437 Variance in reproductive success explains levels of observed genetic 438 diversity

439 To understand the mechanisms by which adult lifespan affects genetic diversity and test if  
440 it can alone explain our results, we built life tables for each of the 16 species by incorporating  
441 age-specific fecundity and survival, age at first maturity, lifespan and sex-specific differences in  
442 these parameters.

443 Non-genetic estimates of  $\frac{N_e}{N}$  ratio obtained with AgeNe ranged from 0.104 in *L. budegassa* to  
444 0.671 for *S. cinereus*. When considering the 16 species together, the  $\frac{N_e}{N}$  ratio was not signifi-  
445 cantly correlated with genetic diversity ( $p$ -value = 0.0935). However, four out of five brooding  
446 species had low genetic diversity despite high  $\frac{N_e}{N}$  ratios (Fig 3A). As previously observed, re-  
447 moving the 5 brooders increased the slope and the percentage of variance of genetic diversity  
448 explained by variance of  $\frac{N_e}{N}$  above null expectations obtained by removing groups of 5 species at  
449 random (slope = 1.849, 95% CI =  $[0.048, 1.582]$ , pseudo- $R^2 = 0.55$ , 95% CI =  $[0.004, 0.533]$ , Fig  
450 S12). Thus, the  $\frac{N_e}{N}$  ratio predicted by life tables was positively correlated to genetic diversity  
451 when considering non-brooding species only (Fig 3A).

Dataset	Predictor	<i>p</i> -value	Pseudo $R^2$	Slope estimate ( $\pm$ 95% interval)
Whole data set	Body size	0.119	0.192	-0.006(-0.014; 0.002)
	Trophic level	0.676	0.012	-0.091(-0.524; 0.343)
	Propagule size	0.562	0.015	-0.014(-0.062; 0.034)
	Fecundity	0.653	0.013	$-1.22e^{-5}$ ( $-6.63e^{-5}$ ; $4.20e^{-5}$ )
	Lifespan	<b>0.0107</b>	0.438	-0.062(-0.111; -0.013)
	Adult lifespan	<b>0.0070</b>	0.429	-0.089(-0.156; -0.023)
	Hermaphroditism	0.434	0.034	0.1779(-0.278; 0.633)
	Parental Care	0.274	0.075	-0.273(-0.772; 0.226)
No parental care	Body size	<b><math>6.60e^{-5}</math></b>	0.616	-0.014(-0.021; -0.007)
	Trophic level	0.256	0.093	-0.326(-0.902; 0.251)
	Propagule size	0.170	0.175	-0.518(-1.273; 0.237)
	Fecundity	0.390	0.056	$-2.51e^{-5}$ ( $-8.35e^{-5}$ ; $3.33e^{-5}$ )
	Lifespan	<b><math>1.017e^{-7}</math></b>	0.851	-0.095(-0.131; -0.060)
	Adult lifespan	<b><math>1.65e^{-7}</math></b>	0.829	-0.129(-0.179; -0.080)
	Hermaphroditism	0.454	0.044	0.206(-0.345; 0.757)

TABLE 1 – **Statistical relationships between species genetic diversity and life history traits** - Genetic diversity was fitted to 6 quantitative (body size, trophic level, propagule size, fecundity, lifespan and adult lifespan) and two qualitative predictors (hermaphroditism and parental care) with a beta regression model using the `betareg` R package (Zeileis and Hothorn, 2002). In the upper part of the table, regressions were performed with the whole dataset, while in the lower part only the 11 non-brooding species were considered.

452 To determine whether life tables alone are able to reproduce the observed variability in  
453 genetic diversity among species, we compared the regression of pairwise-ratios of  $\frac{N_e}{N}$  and ob-  
454 served genetic diversity to the linear model of slope 1 and intercept 0 (i.e., relative differences  
455 in  $\frac{N_e}{N}$  equal relative differences in genetic diversity). Across all species, the slope of the linear  
456 model of the pairwise-ratios of genetic diversity against ratios of  $\frac{N_e}{N}$  was not significantly dif-  
457 ferent from 1 (estimated slope = 0.73;  $sd = 0.31$ ;  $p$ -value = 0.38) but the intercept was different  
458 from 0 (estimated intercept = 0.47;  $sd = 0.20$ ;  $p$ -value = 0.016, Fig 3C). After removing the  
459 5 brooding species, the estimated model was closer to the model with slope equal to 1 (esti-  
460 mated slope = 0.94;  $sd = 0.22$ ;  $p$ -value = 0.80) and intercept equal to 0 (estimated intercept  
461 = 0.15;  $sd = 0.14$ ;  $p$ -value = 0.30, Fig 3D). Thus, the variance in reproductive success induced  
462 by life tables appeared quantitatively sufficient to explain the extent of variation in observed  
463 genetic diversity (Fig 3A) and especially so when excluding brooders.

464 Our next step was to determine the impact of each component of life tables on genetic  
465 diversity (Fig S7-S8). Starting from a null model (model 1, Fig S7A-S8A), in which species life  
466 tables differed only in lifespan, we found that the  $\frac{N_e}{N}$  ratio ranged from 0.558 to 0.733, a variance  
467 much lower than that of observed genetic diversities. Then, adding separately age and maturity  
468 (model 2, Fig S7B-S8B) or age-specific survival (model 3, Fig S7C-S8C) did not better predict  
469 the ratio of observed genetic diversities. But combining only age at maturity and age-specific  
470 survival (model 4, Fig S7D-S8D) and adding age-specific fecundity (model 4-8, Fig S7D-G, Fig  
471 S8D-G) resulted in a better fit, which was further improved considering only species with no  
472 parental care behaviour. Finally, combining these tree parameters together (age at maturity,  
473 age-specific survival, and fecundity, model 8, Fig S7H-S8H) resulted in the best fit for both  
474 the slope and the intercept and for both non-brooding species and the whole data set. Adding  
475 sex-specific differences in life tables didn't improve the fit, however (models 9 to 16, Fig S7I-P  
476 and Fig S8I-P).

477 Our final step was to further explore the role of the variance in reproductive success on  
478 genetic diversity by simulating genetic diversity at mutation-drift equilibrium with the age-  
479 specific vital rates of the 16 species.

480 We simulated a population of 2000 individuals with a mutation rate  $\mu = 1e^{-7}$ . As expected,  
481 including age-specific vital rates decreased the equilibrium level of genetic diversity when  
482 compared with that of a Wright-Fisher scenario. Under Wright-Fisher conditions, genetic diversity  
483 was equal to 0.08% (in line with theoretical expectations :  $\theta = 4N_e\mu$ ). It was reduced to  
484 0.070% in the species with the least effect of age-specific vital rates (*C. galerita*), and down to  
485 0.010% in the species with the greatest effect (*L. budegassa*). Again, simulated genetic diversity  
486 was not correlated to genetic diversity considering all 16 species ( $p$ -value = 0.297, Fig 3B),  
487 but significantly positively correlated within the sub-sample of the 11 non brooding species  
488 ( $p$ -value = 0.0115). The pairwise-ratio of simulated genetic diversity was marginally correlated  
489 to pairwise-ratio of observed genetic diversity for all species ( $p$ -value = 0.0476, Fig 3E), but  
490 highly significantly correlated considering non-brooders species only ( $p$ -value = 0.00357, Fig  
491 3F). Comparing the impact of each component of life tables on genetic diversity, we found similar  
492 results as previously: life tables with only age-specific survival and/or sex-specific differences  
493 could not generate the variance of observed genetic diversities (Fig S9A-B-E-F, Fig S10A-B-E-  
494 F), but simulated genetic diversity resulting from life tables with fecundity increasing with age  
495 fitted well observed genetic diversities (Fig S9C-D-G-H, Fig S10C-D-G-H).

## 496 Life tables drive correlation between lifespan and the $N_e/N$ ratio

497 In order to determine the general effect of life table properties on the relation between adult  
498 lifespan and  $\frac{N_e}{N}$  beyond the case of marine fish, we modeled 16 life tables with age at maturity  
499 and lifespan similar to those observed in our species but with simulated age-specific survival  
500 and fecundity (Fig 4A), under 5 models of fecundity-age relationships.

501 Considering fecundity constant with age, we found a significant relationship between adult  
502 lifespan and  $\frac{N_e}{N}$  for species with type III survivorship curves ( $c < 1$ ) but not for species having  
503 an age-specific survivorship curve constant,  $c$ , superior to 2, including type I species (Fig 4B).  
504 The slope between adult lifespan and  $\frac{N_e}{N}$  was steepest for type III species, reaching -0.053 for  
505  $c = 0.1$ . For  $c < 2$ , the percentage of variation in  $\frac{N_e}{N}$  explained by adult lifespan was higher  
506 than 60%. Interestingly, it reached a maximum for  $c = 1.03$  at 89% and abruptly dropped down  
507 around  $c = 2$  (Fig 4B).

508 Then, we added an exponential increase in fecundity with age, first taking  $f = 0.142$ , which  
509 is close to the empirical estimations for our 16 species (Fig 4B). The slope between adult  
510 lifespan and  $\frac{N_e}{N}$  became steeper for type I and type II species and reached -0.074 for extreme  
511 type III species ( $c = 0.01$ ). When we included this exponential increase of fecundity with age,  
512 the percentage of variation explained was superior for approximately all values of  $c$ , and the  
513 abrupt drop of percentage of variation explained shifted toward higher  $c$  values, around  $c = 3$ .  
514 Interestingly, we found significant positive relationships associated with low slope values when  
515  $c$  became superior to 10 (type I species).

516 Then, we compared values of slope and  $R^2$  for all  $c$  values and for  $f$  ranging from -1 to 1  
517 (Fig 4C-D). The steepest slope between adult lifespan and  $\frac{N_e}{N}$  that we obtained reached -0.076  
518 for extreme type III species ( $c$  around 0.1), and exponential constant,  $f$ , between 0.18 and  
519 0.31. For type III and type II species ( $c < 1$ ), both the slope and the percentage of variation  
520 explained first increased with increasing exponential constant and then decreased. Significant  
521 negative relationships were found for  $c < 1$  for any values of  $f$ , except some extreme values near  
522 -1, whereas no significant relationship was found for  $c > 1$  when  $f$  is negative except for values  
523 of  $c$  near 1 and values of  $f$  near 0. The steepest slope and the highest percentage of variation  
524 explained were obtained for type III species with intermediate values of  $f$  ( $0.1 < f < 0.5$ ) and

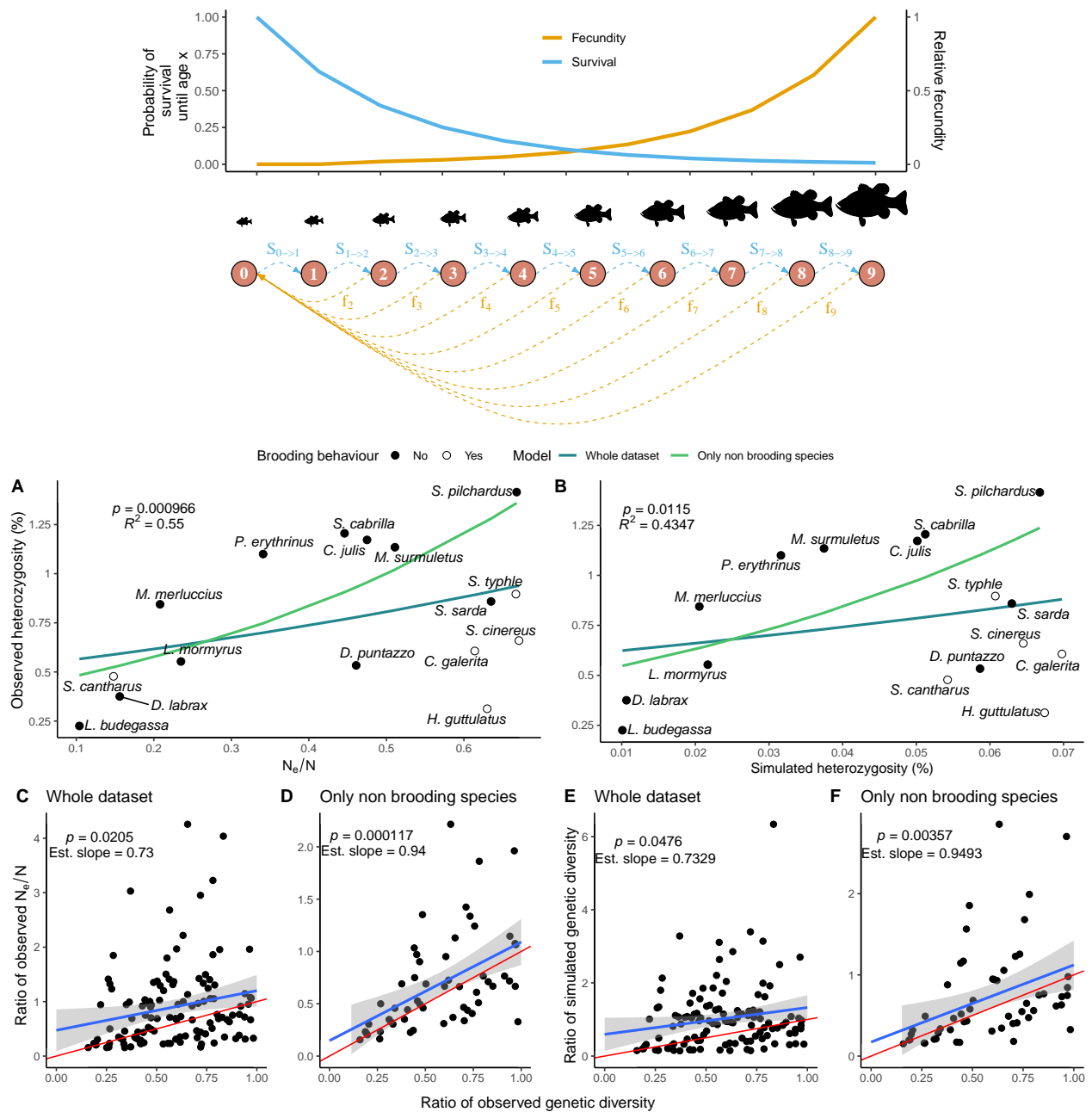


**FIGURE 3 – Variance in reproductive success induced by age-specific vital rates and adult lifespan correlate with observed genetic diversity** - On top, schematic illustration of age-specific fecundity ( $f_{age}$ , in blue) and survival ( $S_{age \rightarrow age+1}$ , yellow) for a simulated species. (A) and (B) represents the relationship between observed genetic diversity on the  $y$ -axis and, respectively,  $\frac{N_e}{N}$  estimated by AgeNe, and simulated genetic diversity with forward-in-time simulations in SLiM v.3.31 (Haller and Messer, 2017), on  $x$ -axis. Life tables containing information on age-specific survival and fecundity and lifespan were used for the 16 species. Age at maturity was used only with AgeNe. Dot points represent non-brooding species and empty circles, brooding species. Blue and green lines represent the beta regression between adult lifespan and genetic diversity considering the whole dataset (16 species), and the 11 non-brooding species only, respectively. The  $p$ -value and the pseudo- $R^2$  are represented on the top left for each of the two top panels for the non-brooders model. Panels (C), (D), (E) and (F) represent the relationships between ratio of observed genetic on  $x$ -axis and, respectively, ratio of  $\frac{N_e}{N}$ , for panels C and D, and ratio of simulated genetic diversity for panels E and F on  $y$ -axis. C and E represents the whole data set, D and F, only the non-brooding species. For each of the four bottom panels, the solid blue lines represents the estimated linear model and the red line, the model with slope 1 and intercept 0. The  $p$ -value and slope estimation is represented on the top-left.



525 for type II species ( $1 < c < 5$ ) for positive values of  $f$ . For type I species, as  $c$  values increased,  
526 higher values of  $f$  are needed to obtain a significant negative relationship between adult lifespan  
527 and the  $\frac{N_e}{N}$  ratio. Above  $c > 20$ , no significant negative relationship was found for any values of  
528  $f$ . Again, we found significant positive relationships and low slopes for  $c > 15$  and intermediate  
529 positive values of  $f$ .

530 We found similar results considering a power-law relationship between age and fecundity,  
531 with slightly less steeper slopes between  $\frac{N_e}{N}$  and adult lifespan, and no significant correlations  
532 for extreme positive values of  $f$  and extreme low values of  $c$ . In contrast, we found limited and  
533 no impact of  $f$  on the relationship between  $\frac{N_e}{N}$  and adult lifespan, respectively, for the linear  
534 and the polynomial age-fecundity model.

## 535 **Historical contingencies explain intra-specific differences in genetic** 536 **diversity**

537 The hierarchical clustering distributed the 16 species in two distinct clusters: the first  
538 one included 9 species with generally lower genetic diversity in Mediterranean than Atlantic  
539 localities, while the opposite was observed in the second cluster (7 species) (Fig 1C). The species  
540 of the second cluster are often found in coastal habitats, lagoons, estuaries whereas species of  
541 the first cluster are rather pelagic, epi-pelagic or benthic species. The only exception was the  
542 presence of *H. guttulatus* in the Atlantic cluster.

## 543 **Discussion**

544 In this study, we used whole-genome high-coverage sequencing data to estimate the genetic  
545 diversity of 16 marine teleost fish with similar geographic distribution ranges. We found that  
546 adult lifespan was the best predictor of genetic diversity, species with long reproductive lifespans  
547 generally having lower genetic diversities (Fig 2). Longevity was already identified as one of  
548 the most important determinants of genetic diversity across Metazoans and plants, in which  
549 it also correlates with the efficacy of purifying selection (Romiguier et al., 2014; Chen et al.,  
550 2017). A positive correlation between longevity and the ratio of nonsynonymous to synonymous  
551 substitutions ( $dN/dS$ ) was also found in teleost fishes (Rolland et al., 2020), thus suggesting  
552 lower  $N_e$  in long-lived species. However, the mechanisms by which lifespan impacts genetic  
553 diversity remain poorly understood and may differ among taxonomic groups. Here we showed  
554 that age-specific fecundity and survival (i.e. vital rates), summarized in life tables, naturally  
555 predict the empirical correlation between adult lifespan and genetic diversity in marine fishes.

## 556 **Impact of life tables on genetic diversity**

557 On a broad taxonomic scale, including plants and animals, Waples et al. (2013) showed  
558 that almost half of the variance in  $\frac{N_e}{N}$  estimated from life tables can be explained with only two  
559 life history traits: age at maturity and adult lifespan. Therefore, the effect of adult lifespan on  
560 genetic diversity should reflect variations in age-specific fecundity and survival across species.  
561 If the species vital rates used to derive  $\frac{N_e}{N}$  ratios are relatively stable over time, the reduction in  
562  $N_e$  due to lifetime variance in reproductive success should not only apply to contemporary time  
563 scales, but more generally throughout the coalescent time. Thus, a direct impact of life tables  
564 on genetic diversity can be expected for iteroparous species with overlapping generations.

565 Using both an analytical (with AgeNe) and a simulation-based (with SLiM) approach, we  
566 showed that age-specific survival and fecundity rates alone can explain a significant fraction of  
567 the variance in genetic diversity among species (Fig 3A-B). This may appear surprising at first  
568 sight, considering that we did not account for among species variation in population census

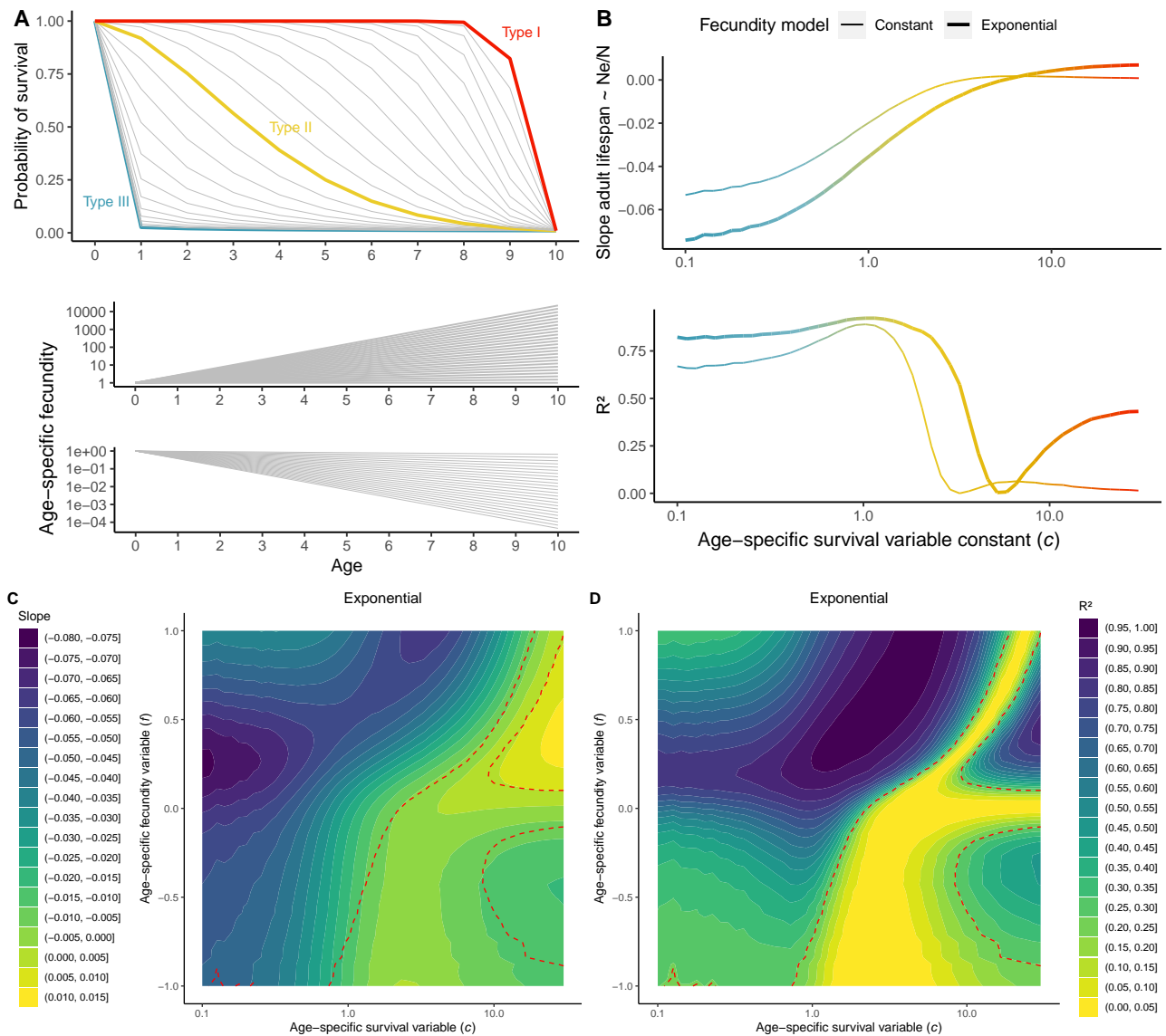


**FIGURE 4 – Slope of the linear model between adult lifespan and  $\frac{N_e}{N}$  ratio estimated with AgeNe for different combinations of age-specific survival and fecundity - A)** On top, gradient of survivorship curves simulated, ranging from type III (blue,  $c < 1$ ), high juvenile mortality and low adult mortality; to type II (orange,  $c$  around 1), constant mortality and type I (red), low juvenile mortality high adult mortality. At the bottom, simulated fecundity either increases or decreases exponentially with age as  $F_{Age} = exp^{f \times Age}$ , with  $f$  ranging from -1 to 1. 16 simulated life tables were constructed with the same values of age at maturity and lifespan as the 16 studied species, and with the corresponding survivorship curve and fecundity-age relationship. **B)** Slope and  $R^2$  of the regression between adult lifespan and  $\frac{N_e}{N}$  ratio for the 16 simulated species as a function of  $c$ , for constant fecundity with age (thin line) and exponential increase of fecundity with age with  $f = 0.14$  (thick line). **C)** Slope and **D)**  $R^2$  of the regression between adult lifespan and  $\frac{N_e}{N}$  ratio for the 16 simulated species for a gradient of values of  $c$  and  $f$ . In **C)**, colder colors indicate steeper slopes; in **D)** higher  $R^2$ .

569 sizes, which vary by several orders of magnitude in marine fishes (Hauser and Carvalho, 2008).  
570 Our results thus support that intrinsic vital rates are crucial demographic components of the  
571 neutral model to understand differences in levels of genetic diversity in marine fishes. But how  
572 generalizable is this finding to other taxa?

573 Age-specific survivorship curves are one of the main biological components of life tables.  
574 Three main types of survivorship curves are classically distinguished: type I curves are charac-  
575 terised by low juvenile and adult mortality combined with an abrupt decrease of survival when  
576 approaching the maximum age (e.g. mammals); in type II curves, survival is relatively constant  
577 during lifetime (e.g. birds) while type III curves are characterised by high juvenile mortality  
578 followed by low adult mortality (e.g. fishes and marine invertebrates). Type III survivorship  
579 curves favor the disproportionate contribution of a few lucky winners that survive to old age,  
580 compared to type I survivorship curves, where individuals have more equal contributions to  
581 reproduction, generating lower variance in reproductive success. Thus, in type III species, hi-  
582 gher lifetime variance in reproductive success is expected as lifespan increases. By simulating  
583 extreme type III survivorship curves ( $c = 0.1$ ) for our 16 species while keeping their true adult  
584 lifespans, we found that  $\frac{N_e}{N}$  can decrease by at most 0.05 per year of lifespan (Fig 4B, extreme  
585 left). This can theoretically induce up to 60% difference in genetic diversity between the species  
586 with the shortest and the longest lifespans of our dataset. In contrast, we found no correlation  
587 between adult lifespan and  $\frac{N_e}{N}$  when simulating type I survivorship curves with the true lifespan  
588 values of the 16 species studied here (Fig 4B,  $c > 2$ ).

589 Another important component of life tables is age-specific fecundity. In marine fishes, fecun-  
590 dity is positively correlated to female ovary size, and the relationship between fecundity and  
591 age is usually well approximated with an exponential ( $F = aexp^{Ab}$ ) or power-law ( $F = aA^b$ )  
592 function. By adding an exponential increase in fecundity with age to our simulations, we found  
593 that  $\frac{N_e}{N}$  decreases even more strongly with increasing adult lifespan ( $\frac{N_e}{N}$  decreases by up to  
594 0.07 per extra year of reproductive life). Using both type III survivorship and exponentially  
595 increasing fecundity with age, we could thus predict up to 84% difference in genetic diversity  
596 between species with the shortest and longest lifespans.

597 Although these predicted relationships were pretty close to our empirical findings, genome-  
598 wide heterozygosity decreased by about 0.09 per additional year of lifespan in our real dataset  
599 (Fig 2), which seems to be a stronger effect compared to theoretical predictions based on vital  
600 rates alone. It is thus likely that other correlates of adult lifespan and unaccounted factors also  
601 contribute to observed differences in genetic diversity among species.

## 602 Correlated effects

603 When relating measures of diversity with the estimates of  $\frac{N_e}{N}$  derived from life tables, we did  
604 not account for differences in census sizes ( $N$ ) among species. Population census sizes can be  
605 huge and are notoriously difficult to estimate in marine fishes. For that reason, abundance data  
606 remain largely unavailable for the 16 species of this study. We nevertheless expect long-lived  
607 species to have lower abundance compared to short-lived species, because in marine fishes  $N$  is  
608 generally negatively correlated to body size, which is itself positively correlated to adult lifespan  
609 in our dataset (Fig S5). Hence, while we have demonstrated here that variation in vital rates  
610 have a direct effect on long-term genetic diversity, the slope between adult lifespan and genetic  
611 diversity may be inflated by uncontrolled variation in  $N$ . Recent genome-wide comparative  
612 studies found negative correlations between  $\frac{N_e}{N}$  and  $N$  in Pinnipeds (Peart et al., 2020) as well  
613 as between genetic diversity and body size in butterflies and birds (Mackintosh et al., 2019;  
614 Brüniche-Olsen et al., 2019). Here, a highly significant negative correlation was found between  
615 genetic diversity and body size and the strength of that correlation was comparable to that  
616 found in a meta-analysis of microsatellite diversity using catch data and body size as proxies



617 for fish abundance (Mccusker and Bentzen, 2010). We note, however, that body size was not  
618 as good a predictor of genetic diversity as lifespan and adult lifespan for the 11 non-brooding  
619 species and it was even not significant in the whole dataset of the 16 species (Table 1).

620 Another potentially confounding effect is the impact of r/K strategies which are the main  
621 determinant of genetic diversity across Metazoans (Romiguier et al., 2014). In our dataset,  
622 fecundity and propagule size (proxies for the r/K gradient) showed only little variance compared  
623 to their range of variation across Metazoans, and none of them were correlated to adult lifespan.  
624 However, we found that the 5 brooding species of our dataset, which are typical K-strategists,  
625 displayed lower genetic diversities with respect to their adult lifespan (Fig 2). Most interestingly,  
626 when these species were removed from the analysis, the effect of adult lifespan on genetic  
627 diversity was amplified, indicating a potentially confounding effect of parental care in marine  
628 fishes. Alternatively, low levels of genetic diversity in brooding species can also be explained by  
629 underestimated lifetime variance in reproductive success by AgeNe due unaccounted variance  
630 in reproductive succes within age-class. This effect could be high for species with strong sexual  
631 selection and mate choice (Hastings, 1988; Naud et al., 2009). Moreover, most of all these species  
632 inhabit lagoons and coastal habitats, corresponding to smaller ecological niches compared to  
633 species with no parental care, thus potentially resulting in lower long-term abundances. The  
634 discrepancy introduced by brooders in the relationship that we observed here between adult  
635 lifespan and genetic diversity may thus involve a variety of effects that remain to be elucidated.

636 Temporal fluctuations of effective population size may also have impacted observed levels  
637 of genetic diversity (Nei et al., 1975). All studied species possibly went through a bottleneck  
638 during the the Last Glacial Maximum (Jenkins et al., 2018), which may have simultaneously de-  
639 creased their genetic diversities. As the time of return to mutation-drift equilibrium is positively  
640 correlated to generation time, which is itself directly linked to adult lifespan, we may expect  
641 long-lived species to have recovered less genetic variation than short-lived species following their  
642 latest bottleneck. Moreover, long-lived species may not have recovered their pre-bottleneck po-  
643 pulation sizes as rapidly as short-lived species. If true, the negative relationship between adult  
644 lifespan and genetic diversity may be inflated compared to the sole effect of life tables.

645 Variation in mutation rates between species could not be accounted for due to a lack of  
646 estimates. However, if species-specific mutation rates were correlated with adult lifespan, we  
647 would expect mutation rate variation to have a direct effect on genetic diversity. Mutation rate  
648 could be linked with species life history traits through three possible mechanisms. First, the  
649 drift-barrier hypothesis predicts a negative correlation between species effective population size  
650 and the per-generation mutation rate (Sung et al., 2012). However, this hypothesis seems in  
651 contradiction with our results since species with the highest effective population sizes have the  
652 highest genetic diversity. Second, species with larger genome size tend to have more germ line  
653 cell divisions, hence possibly higher mutation rates. But we did not find any correlation between  
654 genome size and genetic diversity or any other qualitative and quantitative life history traits.  
655 Third, species with longer generation time, which is positively correlated to lifespan and age at  
656 maturity, may have higher per-generation mutation rate as older individuals accumulate more  
657 germinal mutations through their lives. Again, under this assumption, we would expect species  
658 with longer lifespan, to have higher mutation rate and genetic diversity, which is contrary to  
659 our observations. In summary, variation in mutation rates among species due to differences  
660 in lifespan are unlikely to explain the negative lifespan-diversity relationship we observed. If  
661 anything, variation in mutation rates should theoretically oppose this relationship.

662 Using one of the few direct estimates of the per-generation mutation rate in fish, Feng  
663 et al. (2017) explained the surprisingly low nucleotide diversity found in the Atlantic herring  
664 *Clupea harengus* ( $\pi = 0.3\%$ ) by a very low mutation rate of  $2 \times 10^9$  estimated from pedigree  
665 analysis. Although the herring is one of the most abundant and fecund pelagic species in the  
666 North Atlantic Ocean, its genetic diversity appears approximetaly 80% lower than that of

667 the european pilchard *S. pilchardus*, another member of the *Clupeidae* family that show the  
668 highest diversity in our study. Even if *C. harengus* has a larger body size (approximately 30 cm,  
669 compared to 20 cm for *S. pilchardus*, Froese et al. (2000)), it has above all a much longer lifespan  
670 (between 12 and 25 years) and a later age at maturity (between 2 and 6.5 years) (Jennings and  
671 Beverton, 1991). Considering the even lowest estimate of adult lifespan reported for the herring  
672 (10 years), the corresponding genetic diversity predicted by our model linking adult lifespan to  
673 genetic diversity would be 0.05 %, which is pretty close to the empirical estimate.

674 Finally, we did not take into account the erosion of neutral diversity through linked selec-  
675 tion. Addressing that issue would need to generate local estimates of nucleotide diversity and  
676 population recombination rate along the genome of each species using resequencing data aligned  
677 to a reference assembly, which was out of the scope of this study. The predicted effect of linked  
678 selection would be, however, to remove more diversity in species with large compared to small  
679  $N_e$ . It is therefore likely that linked selection would rather attenuate the negative relationship  
680 between adult lifespan and genetic diversity compared to neutral predictions.

## 681 Conclusion

682 Here we used a simple approach to generate reference-free genome-wide estimates of diversity  
683 with  $k$ -mer analysis. Tested on two species with genetic diversities ranging from 0.22 to 1.42%  
684 the  $k$ -mer approach performed close to the level of a high-standard reference-based method in  
685 capturing fine-scale variation in diversity between evolutionary lineages and even populations  
686 of the same species. This opens the possibility to address the determinants of genetic diversity  
687 in other groups of taxa at limited costs without relying on existing genomics resources. Across  
688 Metazoans, the level of genetic diversity showed no significant relationship with the species'  
689 conservation status (Romiguier et al., 2014). Studies performed at lower phylogenetical scales  
690 such as in Darwin's finches and Pinnipeds, however, found reduced contemporary genetic diver-  
691 sity in threatened compared to non-threatened species (Brüniche-Olsen et al., 2019; Peart et al.,  
692 2020). Our results complement and extend this literature by showing the importance of taking  
693 into account life tables in comparisons of genetic diversity between species. Fish species exposed  
694 to overfishing have been showed to exhibit lower microsatellite diversity compared with other  
695 fish (Pinsky and Palumbi, 2014). By eliminating preferentially the oldest age classes from fish  
696 populations, overfishing may potentially modify life tables towards a decrease in the variance in  
697 reproductive success among individuals. Therefore, fishing may shift the mutation-drift balance  
698 in a counter-intuitive way that could mitigate the effect of decline in abundance on the loss of  
699 polymorphism over the long term.

## 700 Acknowledgments

701 The data used in this work were partly produced with the support of the GenSeq genoty-  
702 ping and sequencing platform, and bioinformatic data analysis benefited from the Montpellier  
703 Bioinformatics Biodiversity MBB platform, both platforms being supported by ANR program  
704 "Investissements d'avenir" (ANR-10-LABX-04-01). We would like to thank Rémy Darnat and  
705 Khalid Belkhir for their invaluable assistance in data storage, management and processing. We  
706 are grateful to the colleagues who provided us with samples as well as to those who facilitated or  
707 participated in sampling : F. Schlichta, T. Pastor, R. Castilho, R. Cunha, R. Lechuga, D. Pilo,  
708 C. Mena, J. Charton, T. Robinet, A. Darnaude, S. Vaz, M. Duranton, N. Bierne, S. Villéger,  
709 S. Blouet, as well as the fishermen and employees of fish markets and fish auctions. This work  
710 was supported by the ANR grant CoGeDiv ANR-17-CE02-0006-01.

## 711 **Author contributions**

712 P.B., T.B. and P.-A.G. wrote the manuscript. P.B. and P.-A.G performed fieldwork. P.B.  
713 performed molecular experiments, and all bioinformatic and evolutionary genomics analyses  
714 with inputs from T.B. and P.-A.G. P.-A.G. conceived the project and managed financial support  
715 and genome sequencing.

## 716 **Data archiving**

717 Data and scripts used in this study are freely available in the GitHub repository [https://](https://github.com/pierrebarry/life_tables_genetic_diversity_marine_fishes)  
718 [github.com/pierrebarry/life\\_tables\\_genetic\\_diversity\\_marine\\_fishes](https://github.com/pierrebarry/life_tables_genetic_diversity_marine_fishes). All sampling  
719 metadata are accessible under GEOME at the CoGeDiv Project Homepage : [https://geome-db.](https://geome-db.org/workbench/project-overview?projectId=357)  
720 [org/workbench/project-overview?projectId=357](https://geome-db.org/workbench/project-overview?projectId=357). Sequence reads have been deposited in  
721 the GenBank Sequence Read Archive under the accession code BioProject PRJNAXXXX.

## 722 **Références**

- 723 Benvenuto, C., Coscia, I., Chopelet, J., Sala-Bozano, M., and Mariani, S. (2017). Ecological  
724 and evolutionary consequences of alternative sex-change pathways in fish. *Scientific Reports*,  
725 7(1) :9084.
- 726 Brüniche-Olsen, A., Kellner, K. F., and DeWoody, J. A. (2019). Island area, body size and  
727 demographic history shape genomic diversity in Darwin’s finches and related tanagers. *Mo-*  
728 *lecular Ecology*, 28(22) :4914–4925.
- 729 Chen, J., Glémin, S., and Lascoux, M. (2017). Genetic Diversity and the Efficacy of Purifying  
730 Selection across Plant and Animal Species. *Molecular Biology and Evolution*, 34(6) :1417–  
731 1428.
- 732 Chen, S., Zhou, Y., Chen, Y., and Gu, J. (2018). Fastp : An ultra-fast all-in-one FASTQ  
733 preprocessor. *Bioinformatics*, 34(17) :i884–i890.
- 734 Cribari-Neto, F. and Zeileis, A. (2010). Beta Regression in R. *Journal of Statistical Software*,  
735 34(1) :1–24.
- 736 Crow, J. F. and Kimura, M. (1970). *An Introduction to Population Genetics Theory*. Harper  
737 & Row.
- 738 Curtis, J. M. R. and Vincent, A. C. J. (2006). Life history of an unusual marine fish : Survival,  
739 growth and movement patterns of *Hippocampus guttulatus* Cuvier 1829. *Journal of Fish*  
740 *Biology*, 68(3) :707–733.
- 741 Danecek, P., Auton, A., Abecasis, G., Albers, C. A., Banks, E., DePristo, M. A., Handsaker,  
742 R. E., Lunter, G., Marth, G. T., Sherry, S. T., McVean, G., and Durbin, R. (2011). The  
743 variant call format and VCFtools. *Bioinformatics*, 27(15) :2156–2158.
- 744 Díez-Del-Molino, D., Sánchez-Barreiro, F., Barnes, I., Gilbert, M. T. P., and Dalén, L. (2018).  
745 Quantifying Temporal Genomic Erosion in Endangered Species. *Trends in Ecology & Evolu-*  
746 *tion*, 33(3) :176–185.
- 747 Domínguez-Seoane, R., Pajuelo, J. G., Lorenzo, J. M., and Ramos, A. G. (2006). Age and  
748 growth of the sharpnose seabream *Diplodus puntazzo* (Cetti, 1777) inhabiting the Cana-  
749 rian archipelago, estimated by reading otoliths and by backcalculation. *Fisheries Research*,  
750 81(2) :142–148.
- 751 Ellegren, H. and Galtier, N. (2016). Determinants of genetic diversity. *Nature Reviews Genetics*,  
752 17(7) :422–433.
- 753 Falconer, D. S. (1989). *Introduction to Quantitative Genetics*. Longman, Scientific & Technical ;  
754 Wiley, Burnt Mill, Harlow, Essex, England : New York, 3rd ed edition.
- 755 Feng, C., Pettersson, M., Lamichhaney, S., Rubin, C.-J., Rafati, N., Casini, M., Folkvord, A.,  
756 and Andersson, L. (2017). Moderate nucleotide diversity in the Atlantic herring is associated  
757 with a low mutation rate. *eLife*, 6 :e23907.
- 758 Frankham, R. (1995). Conservation Genetics. *Annual Review of Genetics*, 29(1) :305–327.
- 759 Froese, R., Pauly, D., and Editors (2000). FishBase 2000 : Concepts, design and data sources.  
760 page 344.

- 761 Gage, T. B. (2001). Age-specific fecundity of mammalian populations : A test of three mathe-  
762 matical models. *Zoo Biology*, 20(6) :487–499.
- 763 Ganas, K., Somarakis, S., Machias, A., and Theodorou, A. J. (2003). Evaluation of spaw-  
764 ning frequency in a Mediterranean sardine population (*Sardina pilchardus sardina*). *Marine*  
765 *Biology*, 142(6) :1169–1179.
- 766 Haller, B. C. and Messer, P. W. (2017). SLiM 2 : Flexible, Interactive Forward Genetic Simu-  
767 lations. *Molecular Biology and Evolution*, 34(1) :230–240.
- 768 Hastings, P. A. (1988). Female choice and male reproductive success in the angel blenny,  
769 *Coralliozetus angelica* (Teleostei : Chaenopsidae). *Animal Behaviour*, 36(1) :115–124.
- 770 Hauser, L. and Carvalho, G. R. (2008). Paradigm shifts in marine fisheries genetics : Ugly  
771 hypotheses slain by beautiful facts. *Fish and Fisheries*, 9(4) :333–362.
- 772 Hedgecock, D. (1994). Does variance in reproductive success limit effective population sizes of  
773 marine organisms? In A. *Genetics and Evolution of Aquatic Organisms*.
- 774 Hedgecock, D. and Pudovkin, A. I. (2011). Sweepstakes Reproductive Success in Highly Fe-  
775 cund Marine Fish and Shellfish : A Review and Commentary. *Bulletin of Marine Science*,  
776 87(4) :971–1002.
- 777 Hedrick, P. (2005). Large variance in reproductive success and the  $N_e/N$  ratio. *Evolution*,  
778 59(7) :1596–1599.
- 779 Iglésias, S. (2013). *Actinopterygians from the North-Eastern Atlantic and the Mediterranean (A*  
780 *Natural Classification Based on Collection Specimens, with DNA Barcodes and Standardized*  
781 *Photographs), Volume I (Plates), Provisional Version 09*.
- 782 Jenkins, T. L., Castilho, R., and Stevens, J. R. (2018). Meta-analysis of northeast Atlantic  
783 marine taxa shows contrasting phylogeographic patterns following post-LGM expansions.  
784 *PeerJ*, 6 :e5684.
- 785 Jennings, S. and Beverton, R. J. H. (1991). Intraspecific variation in the life history tactics of  
786 Atlantic herring (*Clupea harengus* L.) stocks. *ICES Journal of Marine Science*, 48(1) :117–  
787 125.
- 788 Kimura, M. (1983). *The Neutral Theory of Molecular Evolution*. Cambridge University Press,  
789 Cambridge.
- 790 Kimura, M. and Crow, J. F. (1964). The Number of Alleles That Can Be Maintained in a  
791 Finite Population. *Genetics*, 49(4) :725–738.
- 792 Kraljević, M., Matić-Skoko, S., Dul\vcic, J., Pallaoro, A., Jardas, I., and Glamuzina, B. (2007).  
793 Age and growth of sharpsnout seabream *Diplodus puntazzo* (Cetti, 1777) in the eastern  
794 Adriatic Sea.
- 795 Lande, R. (1995). Mutation and Conservation. *Conservation Biology*, 9(4) :782–791.
- 796 Lande, R. and Barrowclough, G. F. (1987). Effective population size, genetic variation, and their  
797 use in population management. In Soulé, M. E., editor, *Viable Populations for Conservation*,  
798 pages 87–124. Cambridge University Press, Cambridge.



- 799 Leffler, E. M., Bullaughey, K., Matute, D. R., Meyer, W. K., Ségurel, L., Venkat, A., Andolfatto,  
800 P., and Przeworski, M. (2012). Revisiting an Old Riddle : What Determines Genetic Diversity  
801 Levels within Species? *PLOS Biology*, 10(9) :e1001388.
- 802 Leroy, T., Rousselle, M., Tilak, M.-K., Caizergues, A., Scornavacca, C., Carrasco, M. R., Fuchs,  
803 J., Illera, J. C., Swardt, D. H. D., Thébaud, C., Milà, B., and Nabholz, B. (2020). Endemic  
804 island songbirds as windows into evolution in small effective population sizes. *bioRxiv*, page  
805 2020.04.07.030155.
- 806 Lewontin, R. C. (1974). *The Genetic Basis of Evolutionary Change*. Number 25 in Columbia  
807 Biological Series. Columbia Univ. Pr, New York.
- 808 Li, H. and Durbin, R. (2009). Fast and accurate short read alignment with Burrows-Wheeler  
809 transform. *Bioinformatics (Oxford, England)*, 25(14) :1754–1760.
- 810 Louro, B., De Moro, G., Garcia, C., Cox, C. J., Veríssimo, A., Sabatino, S. J., Santos, A. M.,  
811 and Canário, A. V. M. (2019). A haplotype-resolved draft genome of the European sardine  
812 (*Sardina pilchardus*). *GigaScience*, 8(5).
- 813 Mackintosh, A., Laetsch, D. R., Hayward, A., Charlesworth, B., Waterfall, M., Vila, R., and  
814 Lohse, K. (2019). The determinants of genetic diversity in butterflies. *Nature Communica-*  
815 *tions*, 10(1) :1–9.
- 816 Marçais, G. and Kingsford, C. (2011). A fast, lock-free approach for efficient parallel counting  
817 of occurrences of k-mers. *Bioinformatics*, 27(6) :764–770.
- 818 Martinez, A. S., Willoughby, J. R., and Christie, M. R. (2018). Genetic diversity in fishes is  
819 influenced by habitat type and life-history variation. *Ecology and Evolution*, 8(23) :12022–  
820 12031.
- 821 Mccusker, M. R. and Bentzen, P. (2010). Positive relationships between genetic diversity and  
822 abundance in fishes. *Molecular Ecology*, 19(22) :4852–4862.
- 823 Milton, P. (1983). Biology of littoral blennioid fishes on the coast of south-west England. *Journal*  
824 *of the Marine Biological Association of the United Kingdom*, 63(1) :223–237.
- 825 Murua, H. and Motos, L. (2006). Reproductive strategy and spawning activity of the European  
826 hake *Merluccius merluccius* (L.) in the Bay of Biscay. *Journal of Fish Biology*, 69(5) :1288–  
827 1303.
- 828 Naud, M.-J., Curtis, J. M. R., Woodall, L. C., and Gaspar, M. B. (2009). Mate choice, ope-  
829 rational sex ratio, and social promiscuity in a wild population of the long-snouted seahorse  
830 *Hippocampus guttulatus*. *Behavioral Ecology*, 20(1) :160–164.
- 831 Nei, M., Maruyama, T., and Chakraborty, R. (1975). The Bottleneck Effect and Genetic  
832 Variability in Populations. *Evolution*, 29(1) :1.
- 833 Nunney, L. (1991). The Influence of Age Structure and Fecundity on Effective Population Size.  
834 *Proceedings : Biological Sciences*, 246(1315) :71–76.
- 835 Nunney, L. (1996). The influence of variation in female fecundity on effective population size.  
836 *Biological Journal of the Linnean Society*, 59(4) :411–425.

- 837 Pauly, D., Morgan, G. R., International Center for Living Aquatic Resources Management, and  
838 Ma'had al-Kuwayt lil-Abḥāth al-'Ilmiyah, editors (1987). *Length-Based Methods in Fisheries*  
839 *Research*. Number no. 325 in ICLARM Contribution. International Center for Living Aquatic  
840 Resources Management; Kuwait Institute for Scientific Research, Makati, Metro Manila,  
841 Philippines : Safat, Kuwait.
- 842 Peart, C. R., Tusso, S., Pophaly, S. D., Botero-Castro, F., Wu, C.-C., Auriolles-Gamboa, D.,  
843 Baird, A. B., Bickham, J. W., Forcada, J., Galimberti, F., Gemmell, N. J., Hoffman, J. I.,  
844 Kovacs, K. M., Kunnsaranta, M., Lydersen, C., Nyman, T., de Oliveira, L. R., Orr, A. J.,  
845 Sanvito, S., Valtonen, M., Shafer, A. B. A., and Wolf, J. B. W. (2020). Determinants of  
846 genetic variation across eco-evolutionary scales in pinnipeds. *Nature Ecology & Evolution*,  
847 pages 1–10.
- 848 Pinder, J. E., Wiener, J. G., and Smith, M. H. (1978). The Weibull Distribution : A New  
849 Method of Summarizing Survivorship Data. *Ecology*, 59(1) :175–179.
- 850 Pinsky, M. L. and Palumbi, S. R. (2014). Meta-analysis reveals lower genetic diversity in  
851 overfished populations. *Molecular Ecology*, 23(1) :29–39.
- 852 Poplin, R., Ruano-Rubio, V., DePristo, M. A., Fennell, T. J., Carneiro, M. O., der Auwera, G.  
853 A. V., Kling, D. E., Gauthier, L. D., Levy-Moonshine, A., Roazen, D., Shakir, K., Thibault,  
854 J., Chandran, S., Whelan, C., Lek, M., Gabriel, S., Daly, M. J., Neale, B., MacArthur, D. G.,  
855 and Banks, E. (2018). Scaling accurate genetic variant discovery to tens of thousands of  
856 samples. *bioRxiv*, page 201178.
- 857 Ricklefs, R. E. and Miller, G. L. (1999). *Ecology*. W.H.Freeman & Co Ltd, New York, 4th  
858 edition edition.
- 859 Rolland, J., Schluter, D., and Romiguier, J. (2020). Vulnerability to Fishing and Life History  
860 Traits Correlate with the Load of Deleterious Mutations in Teleosts. *Molecular Biology and*  
861 *Evolution*.
- 862 Romiguier, J., Gayral, P., Ballenghien, M., Bernard, A., Cahais, V., Chenuil, A., Chiari, Y.,  
863 Dernet, R., Duret, L., Faivre, N., Loire, E., Lourenco, J. M., Nabholz, B., Roux, C., Tsagko-  
864 georga, G., a. T. Weber, A., Weinert, L. A., Belkhir, K., Bierne, N., Glémin, S., and Galtier,  
865 N. (2014). Comparative population genomics in animals uncovers the determinants of genetic  
866 diversity. *Nature*, 515(7526) :261–263.
- 867 Sung, W., Ackerman, M. S., Miller, S. F., Doak, T. G., and Lynch, M. (2012). Drift-barrier  
868 hypothesis and mutation-rate evolution. *Proceedings of the National Academy of Sciences*,  
869 109(45) :18488–18492.
- 870 Tine, M., Kuhl, H., Gagnaire, P.-A., Louro, B., Desmarais, E., Martins, R. S. T., Hecht, J.,  
871 Knaust, F., Belkhir, K., Klages, S., Dieterich, R., Stueber, K., Piferrer, F., Guinand, B.,  
872 Bierne, N., Volckaert, F. A. M., Bargelloni, L., Power, D. M., Bonhomme, F., Canario, A.  
873 V. M., and Reinhardt, R. (2014). European sea bass genome and its variation provide insights  
874 into adaptation to euryhalinity and speciation. *Nature Communications*, 5 :5770.
- 875 Tsikliras, A. C. and Stergiou, K. I. (2015). Age at maturity of Mediterranean marine fishes.  
876 *Mediterranean Marine Science*, 16(1) :5–20.
- 877 Väli, Ü., Einarsson, A., Waits, L., and Ellegren, H. (2008). To what extent do microsatellite  
878 markers reflect genome-wide genetic diversity in natural populations? *Molecular Ecology*,  
879 17(17) :3808–3817.

- 880 Vurture, G. W., Sedlazeck, F. J., Nattestad, M., Underwood, C. J., Fang, H., Gurtowski, J.,  
881 and Schatz, M. C. (2017). GenomeScope : Fast reference-free genome profiling from short  
882 reads. *Bioinformatics*, 33(14) :2202–2204.
- 883 Waples, R. S. (1991). Heterozygosity and Life-History Variation in Bony Fishes : An Alternative  
884 View. *Evolution*, 45(5) :1275–1280.
- 885 Waples, R. S. (2002). Evaluating the effect of stage-specific survivorship on the  $N_e/N$  ratio.  
886 *Molecular Ecology*, 11(6) :1029–1037.
- 887 Waples, R. S. (2016a). Life-history traits and effective population size in species with overlap-  
888 ping generations revisited. *Heredity*, 117(4) :241–250.
- 889 Waples, R. S. (2016b). Tiny estimates of the  $N_e/N$  ratio in marine fishes : Are they real?  
890 *Journal of Fish Biology*, 89(6) :2479–2504.
- 891 Waples, R. S., Do, C., and Chopelet, J. (2011). Calculating  $N_e$  and  $N_e/N$  in age-structured  
892 populations : A hybrid Felsenstein-Hill approach. *Ecology*, 92(7) :1513–1522.
- 893 Waples, R. S., Luikart, G., Faulkner, J. R., and Tallmon, D. A. (2013). Simple life-history  
894 traits explain key effective population size ratios across diverse taxa. *Proceedings of the*  
895 *Royal Society B : Biological Sciences*, 280(1768).
- 896 Waples, R. S., Mariani, S., and Benvenuto, C. (2018). Consequences of sex change for effective  
897 population size. *Proceedings of the Royal Society B : Biological Sciences*, 285(1893) :20181702.
- 898 White, E. P., Ernest, S. K. M., Kerkhoff, A. J., and Enquist, B. J. (2007). Relationships between  
899 body size and abundance in ecology. *Trends in Ecology & Evolution*, 22(6) :323–330.
- 900 Wright, S. (1969). *The Theory of Gene Frequencies*. Number Sewall Wright ; Vol. 2 in *Evolution*  
901 and the Genetics of Populations. Univ. of Chicago Press, Chicago, Ill., paperback ed edition.
- 902 Zeileis, A. and Hothorn, T. (2002). Diagnostic checking in regression relationships. *R News*,  
903 2(3) :7–10.